Chemical Engineering Journal 165 (2010) 111–116

Contents lists available at ScienceDirect

Chemical Engineering Journal

journal homepage: www.elsevier.com/locate/cej

Decolorization of Acid Red 1 dye solution by Fenton-like process using Fe–Montmorillonite K10 catalyst

N.K. Daud, M.A. Ahmad, B.H. Hameed*

School of Chemical Engineering, Engineering Campus, Universiti Sains Malaysia, 14300 Nibong Tebal, Penang, Malaysia

ARTICLE INFO

Article history:
Received 9 February 2010
Received in revised form 28 August 2010
Accepted 31 August 2010

Keywords:
Decolorization
Fenton-like process
Acid Red 1
Fe–Montmorillonite K10

ABSTRACT

In this work, the decolorization of Acid Red 1 (AR1) dye was conducted using Fe(III) oxide immobilized on Montmorillonite K10 (Fe–MK10) catalyst in the presence of hydrogen peroxide (H_2O_2) in batch process. The effects of different parameters such as iron loading (Fe^{3+}) on Montmorillonite K10 (MK10), catalyst dosage, solution pH, initial concentration of H_2O_2 and AR1 and reaction temperature on the decolorization efficiency of the process were studied. The results indicated that by using 5.0 g L^{-1} catalyst dosage of 0.14 wt.% Fe–MK10 at pH 2.5 and 16 mM of H_2O_2, 99% of the 50 mg L^{-1} of AR1 was decolorized within 150 min. Leaching test indicated that the leached iron from the catalyst was less than 5 mg L^{-1}.

1. Introduction

Water pollution is a major problem in the global context. Chemical process industries, such as oil refineries, petrochemical units, dye and dye intermediate manufacturing industries, textile units, among others, are typical industries that dump toxic organic compounds to the nearer water courses, thus causing sever pollution [1]. Amongst them, the dye and dye intermediate manufacturing and textile industries stand out as they produce a large amount of effluents which can cause serious environmental problems as they contain colored compounds resulting from dyes unfixed to fibers during the dyeing process [2].

The effluents discharged from these industries are usually strongly colored, and the direct release of the wastewater into receiving water body will cause damage to both aquatic life and human beings due to their toxic, carcinogenic and mutagenic effects [3,4]. Actually, the removal of dyes from wastewater is a challenge to the related industries, because the synthetic dyes used are stable compounds and difficult to destroy by common treatments. Physical, chemical, and biological methods are presently available for the treatment of wastewater discharged from various industries [5]. However, physical methods such as liquid–liquid extraction, ion-exchange, adsorption, air or steam stripping, etc., are ineffective on pollutants which are not readily adsorbable or volatile, and have further disadvantages because they simply transfer the pollutants to another phase rather than destroying them [6].

Acid dyes are a type of azo dyes, that are characterized by the presence of one or more azo groups (–N=N–) bound to aromatic rings and the largest and most important class of synthetic organic dyes. It has been estimated that more than 50% of all dyes in common use are azo dyes because of their chemical stability and versatility [7,8]. The complex molecular structures of most azo dyes make them resistant to biological or even chemical degradation. This also renders the conventional physical, chemical, and biological treatment methods insufficient and costly for their removal from water [9].

Advanced oxidation processes (AOPs) have been widely proposed, as they operate at temperature near ambient and atmospheric pressure [10]. Hydroxyl radicals (•OH), highly reactive species generated in sufficient quantities by these systems, have the ability to oxidize the majority organic constituents in industrial effluents [11,12]. Common AOPs involve Fenton and photo-Fenton processes, ozonation, electrochemical oxidation, photolysis with H_2O_2 and O_3, high-voltage electrical discharge process, TiO_2 photocatalysis, radiolysis, water solution treatment by electronic beams or γ beams and various combinations of these methods [13–15].

Fenton reaction employed in wastewater treatment processes are known to be very effective in the removal of many hazardous organic pollutants from water [16,17]. Fenton's reagent was discovered about 100 years ago, but its application as an oxidizing process for destroying toxic organics was not applied until the late 1960s [18]. The key step in the Fenton type reaction is the formation of hydroxyl radicals (HO•) from H_2O_2 and Fe(II). It is known that the systems of Fenton type are responsible for oxidation of different organic materials, but their usage as catalysts induces an additional pollution [19–21].

* Corresponding author. Tel.: +60 45996422; fax: +60 45941013.
E-mail address: chbassim@eng.usm.my (B.H. Hameed).

1385-8947/$ – see front matter © 2010 Elsevier B.V. All rights reserved.
doi:10.1016/j.cej.2010.08.072

To overcome the disadvantages of homogeneous Fenton process, heterogeneous Fenton and Fenton-like catalysts have recently received much attention [19]. In a previous work [22,23] we reported the decolorization of Acid Red 1 and reactive black 5 using rice husk-based catalyst and iron–Montmorillonite K10 catalyst, respectively. The objective of this work was to investigate the applicability of Fe(III) oxide contained Montmorillonite K10 (MK10) as heterogeneous Fenton catalyst for decolorization of Acid Red 1 (AR1). The effects of different parameters such as different loading of ferric iron on Montmorillonite K10 (MK10), catalyst dosage, initial concentration of dye and H_2O_2 and initial pH and temperature on the decolorization efficiency of the process were studied.

2. Materials and methods

2.1. Chemicals and reagents

The azo dye, Acid Red 1 (AR1) was obtained from Sigma–Aldrich as commercially available dye and used without further purification. Hydrogen peroxide (H_2O_2) (30%, w/w) and Montmorillonite K10 (MK10) were purchased from Sigma–Aldrich (M) Sdn Bhd, Malaysia. Distilled water was used throughout this study.

2.2. Preparation of Fe–MK10 catalyst

The Fe–MK10 catalyst was prepared by the impregnation method [24], in which distilled water is used to solubilize the ferric nitrate nonahydrate ($Fe(NO_3)_3{\cdot}9H_2O$) (Merck). Then, MK10 was added to this aqueous solution and was stirred constantly in the water-bath until all water was evaporated. After impregnation, the sample was dried at 105 °C for 12 h, followed by calcination at 500 °C for 4 h in a muffle furnace [23].

2.3. Catalyst characterization

Elemental chemical analyses were performed using Energy Dispersive X-ray (EDX) spectroscopy to determine the composition of the original clay and the exact amount of iron in the final catalyst. The morphology of the MK10 was studied using scanning electronic microscopy (SEM) (SEM-JEOL-JSM6301-F) with an Oxford INCA/ENERGY-350 microanalysis system. Fourier Transform Infrared (FT-IR) spectra were recorded in the 4000–400 cm^{-1} region with a PerkinElmer 1730 FT-IR spectrometer, using a He–Ne laser source in KBr pellet (1 mg sample with 300 mg KBr) and 15 scan per minute to improve the signal-to-noise ratio.

Brunauer–Emmett–Teller (BET) specific surface area was determined by adsorption of nitrogen at 77 K using a Micromeritics, ASAP 2020 surface area and porosity analyzer. The X-ray diffraction (XRD) patterns of the catalyst (before and after impregnation) were measured with SIEMENS XRD D5000 equipped with Cu Kα radiation.

2.4. Experimental procedure

Experimental runs were carried out in batch mode using conical flasks filled with 200 mL of the AR1 solution at a given concentration (25–100 mg L^{-1}). In a typical run, the reaction suspension was prepared by adding a given amount of catalyst into solution which has been adjusted to the desired pH value by NaOH or H_2SO_4. The reactions commenced when predetermined amounts of H_2O_2 solution were added to the flasks. Thereafter, samples were withdrawn periodically and analyzed using a UV–vis spectrophotometer. After filtration through 0.42 μm Millipore membrane filters to remove suspended particles. At each stage, the samples withdrawn were returned into the conical flasks.

Table 1
Chemical compositions of MK10 and Fe–MK10 determined by EDX.

Element	Concentration (wt.%)	
	MK10	Fe–MK10
O	40.42	40.46
Fe	8.26	8.48
Al	11.50	10.57
Si	39.82	40.49

2.5. Analytical methods

The concentration of AR1 was analyzed on UV–vis spectrophotometer (Shimadzu, model UV 1601, Japan) with its adsorption at 532 nm, which is the maximum absorption wavelength of AR1. Because the reaction continued after sampling, the measurement of absorbance of reaction solution was done within one min. The decolorization efficiency of AR1 is defined as follows:

$$\text{decolorization efficiency}\,(\%) = \left[1 - \left(\frac{C_t}{C_0}\right)\right] \times 100 \quad (1)$$

where C_0 (mg L^{-1}) is the initial concentration of AR1 and C_t (mg L^{-1}) is the concentration of AR1 at reaction time, t (min).

The total Fe in the solution was determined using Atomic Absorption Spectrophotometer (AAS) model (Shimadzu AA 6650) with the maximum absorbance wavelength (λ_{max}) of iron ion (III) of 248.35 nm. After the decolorization of AR1 was completed, the samples were analyzed to determine the total iron ion leached from the catalyst [23].

3. Results and discussion

3.1. Catalyst characterization

The chemical composition of the 0.14 wt.% Fe–MK10 and MK10 were measured by EDX and are the results are presented in Table 1. The results show that the major elements in MK10 and impregnated MK10 are Si, O, Fe and Al and revealed that the Fe concentration of the Fe–MK10 catalyst is 8.48 wt.%, while it is only 8.26 wt.% in MK10. The distinction of percent by weight of Fe in impregnated MK10 is about 0.22%. Fe was introduced into the clay layers after impregnation method. Slight variations are noticed between the expected and the determined iron content of the samples, which is due to the high hydration degree of the solids at the stages of the preparation procedure, thus making it difficult to obtain the targeted iron contents. The experimental error of the results was determined and represents about 2.6% of uncertainty. Whereas for Si, O and Al, the changes of composition by weight percent occurred about 0.67 wt.%, 0.040 wt.% and 0.93 wt.%, respectively due to the agglomeration of components because of the impregnation of MK10. The reason for using the best loading assayed (0.14 wt.%) was due to the limitation of the iron ions leaching from the support of catalyst that followed the Environmental Quality (Sewage and Industrial Effluents) Regulation 1979 (must below than 5 mg L^{-1}).

Fig. 1 shows the SEM images of MK10 and 0.14 wt.% Fe–MK10. The card-like pattern of the clay mineral layers is seen and not much change on the morphology can be visualized although after MK10 was impregnated with Fe.

FT-IR spectra (4000–400 cm^{-1}) of the MK10, 0.14 wt.% Fe–MK10 and 0.14 wt.% Fe–MK10 after decolorization of AR1 are presented in Fig. 2. Comparing the spectrum of pure MK10 with the spectrum of Fe–MK10, two peaks were depressed at 3629 cm^{-1} and 526 cm^{-1} and one new peak emerged at 1384 cm^{-1} [25]. The former was the NO_3^- stretching mode, which showed that there was some redundant positively charged iron aggregates outside the interlayer space of Fe–MK10 [26], while the latter was the FeOOH bending vibra-

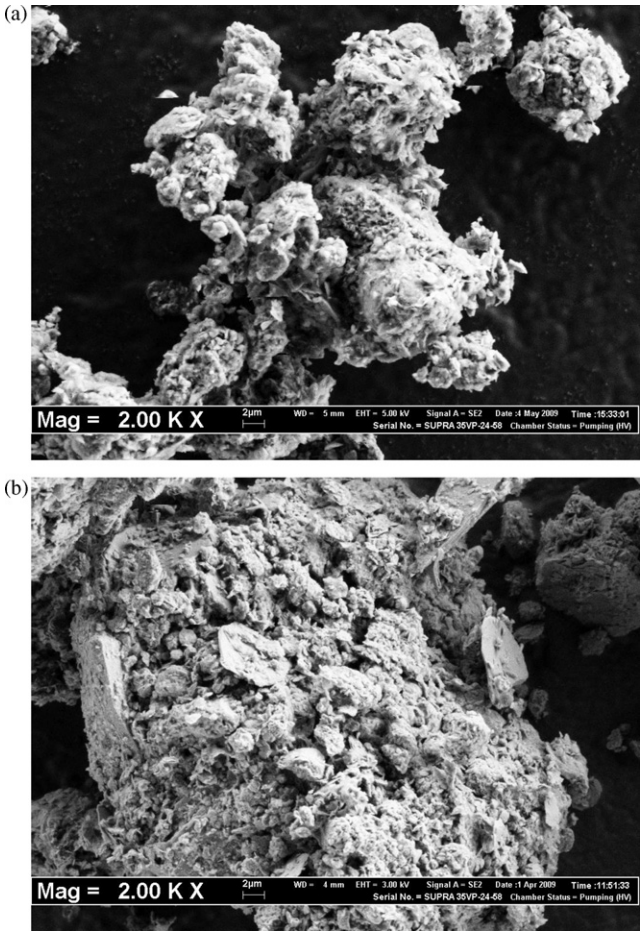

Fig. 1. SEM images of (a) MK10 and (b) 0.14 wt.% of Fe–MK10 (magnification: 2000×).

tion, which also suggested that hydrolyzed iron intercalated into inter layers proceeded by pillaring [27]. Infrared spectra from the MK10 presented peak at 3629 cm^{-1} corresponding to the stretching of hydroxyls groups and cations from the octahedral sheet. Strong bands at 3422–3442 cm^{-1} are indicative of water adsorbed on the MK10 surface, and its presence was confirmed by the deformation band at 1637–1635 cm^{-1}. Bands at 1055 cm^{-1} and 1047 cm^{-1} can be assigned to stretching vibrations of silica–oxygen tetrahedrons as (Si–O–Si). The band at 470 cm^{-1} can be attributed to the bending (Si–O) and stretching (M–O) vibrations. The shift of band at 1047 cm^{-1} and disappear and/or decrease in the intensities of bands of deformation of Al_2OH at 800–900 cm^{-1} and 500–700 cm^{-1}

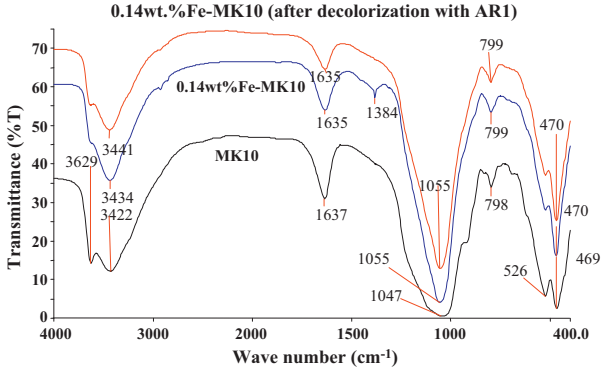

Fig. 2. FT-IR spectra of the samples.

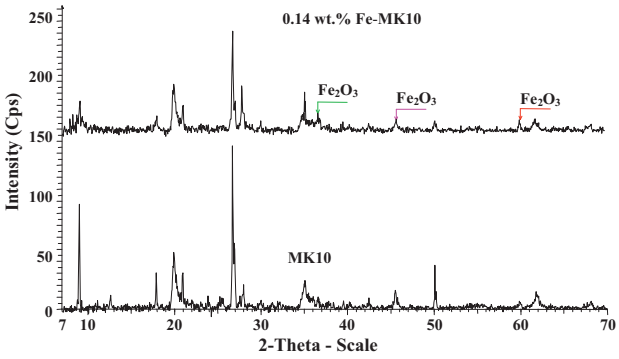

Fig. 3. XRD diffractograms of the samples.

(Si–O), (M–O) and Si–O–Al (octahedral Al) can be indirect evidence of the incorporation of Fe^{3+} into clay [28,29].

BET surface area, pore volume and pore size of 0.14 wt.% Fe–MK10 are 185.434 $m^2\ g^{-1}$, 0.274 $cm^3\ g^{-1}$ and 59 Å, respectively.

Fig. 3 shows the XRD diffractograms of MK10 and impregnated MK10. It can be seen that the impregnated MK10 maintains the layered structure in crystalline form with sodium and quartz-rich elements, but with a remarkable loss of ordering if compared to the MK10 itself. This catalyst, once calcined at 500 °C, show a weak diffraction peaks at $2\theta = 9°$, 18° and 50°. On the other hand, it may be underlined that no peaks due to iron phases are observed in the diffractograms [30]. However, small peaks of anhydrous (Fe_2O_3) oxides were formed after calcinations of the impregnated MK10 by the removal of the organic moieties [31]. This component is indicative of the presence of iron in the impregnated catalyst.

3.2. Role of catalyst support

Before the study on parameters that influence the decolorization process, it is important to evaluate the AR1 decolorization process, i.e., if decolorization occurs through adsorption, through a catalytic reaction or through both processes. The first run was a blank, carried out to evaluate the ability of H_2O_2 or iron ion to decolorize AR1 in aqueous solutions without the addition of any heterogeneous catalyst. Fig. 4 shows the efficiency of AR1 decolorization due to hydrogen peroxide or iron ion is almost negligible (<4% within 150 min), and could be attributed to its low oxidation potential as compared to hydroxyl or perhydroxyl radicals [32]. To determine the influence of the adsorption processes, experiments without H_2O_2 were also carried out. Fig. 4 shows that MK10 as a catalyst support has a low adsorption capacity (6.2% decolorization of dye within 150 min of reaction).

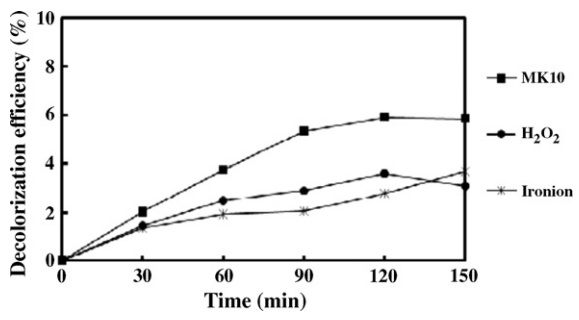

Fig. 4. Un-catalyzed AR1 dye solutions removal by H_2O_2 (4 mM), iron ion (0.05 mM) and adsorption on MK10 (2.0 g L^{-1}).

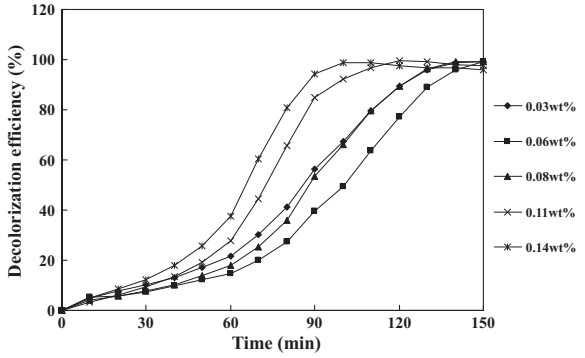

Fig. 5. Effect of iron loading on MK10 on the decolorization of AR1. *Reaction conditions*: initial concentration of AR1, $[AR1]_0 = 50\,mg\,L^{-1}$; initial concentration of hydrogen peroxide, $[H_2O_2]_0 = 4\,mM$; pH 2.5; dosage of catalyst = $2.0\,g\,L^{-1}$; temperature = 30 °C; and agitation speed = 130 rpm.

3.3. Effects of different parameters

Fig. 5 shows the effect of iron loading on MK10. The most fast decolorization efficiency was 0.14 wt.% of Fe^{3+} loading with a value of 99% observed within 150 min reaction. Hence, 0.14 wt.% of Fe^{3+} loading was selected to be the best loading assayed for maximum efficiency. It is important to remark that all decolorization curves in Fig. 5 show a sigmoidal profile, which is typical for autocatalytic or radical reactions. Basically two regions can be identified, the initial one representing the induction period, and the second one after the inflection point representing the steady state [31].

The influence of the catalyst dosage on decolorization efficiency against time is presented in Fig. 6. The efficiency of decolorization within 150 min was 99% with a dosage of $2\,g\,L^{-1}$ until $5\,g\,L^{-1}$ but the kinetics of decolorization was better with high concentration of catalyst. An increase of the concentration of catalyst will increase the amount of Fe ions involved in the process, which in turn increase the number of hydroxyl radical significantly.

The influence of initial pH of the dye solution on the Fe–MK10/H_2O_2 process efficiency was studied using seven solutions with initial pH of 1.5, 2.0, 2.5, 3.0, 3.5, 4.0 and 5.0 and without any modifications or control of pH during the process. Fig. 7 shows the decolorization of dye as a function of the initial pH of the solution at various reaction times. The results indicate that the decolorization of AR1 was significantly influenced by the solution pH and the best solution of pH assayed was observed at 2.5. A similar result was reported in literature [22].

Fig. 8 shows the decolorization of dye as a function of the H_2O_2 concentration of the solution at various reaction times and the

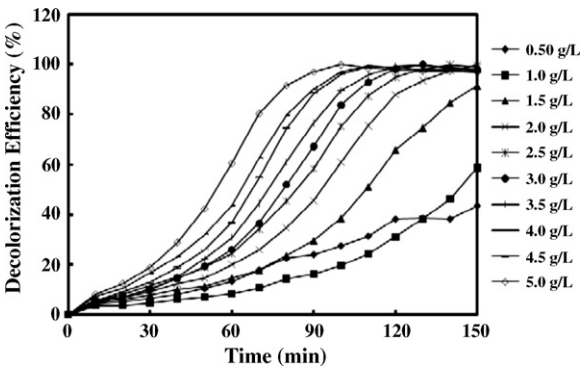

Fig. 6. Effect of dosage of catalyst on the decolorization of AR1. *Reaction condition*: initial concentration of AR1, $[AR1]_0 = 50\,mg\,L^{-1}$; initial concentration of hydrogen peroxide, $[H_2O_2]_0 = 4\,mM$; pH 2.5; 0.14 wt.% of iron ions in catalyst; temperature = 30 °C; and agitation speed = 130.

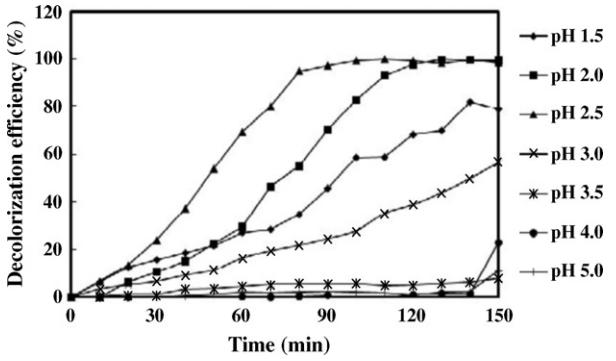

Fig. 7. Effect of pH on the decolorization of AR1. *Reaction conditions*: initial concentration of AR1, $[AR1]_0 = 50\,mg\,L^{-1}$; initial concentration of hydrogen peroxide, $[H_2O_2]_0 = 4\,mM$; dosage of catalyst = $5.0\,g\,L^{-1}$ with 0.14 wt.% of iron ions in catalyst; temperature = 30 °C; and agitation speed = 130 rpm.

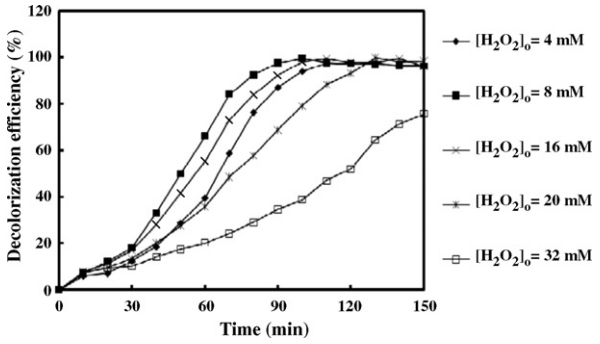

Fig. 8. Effect of initial concentration of H_2O_2 on the decolorization of AR1. *Reaction conditions*: initial concentration of AR1, $[AR1]_0 = 50\,mg\,L^{-1}$; dosage of catalyst = $5.0\,g\,L^{-1}$ with 0.14 wt.% of iron ions in catalyst; temperature = 30 °C; agitation speed = 130 rpm; and pH 2.5.

results showed that 8 mM was the best concentration of H_2O_2 assayed when the initial concentration of AR1 was $50\,mg\,L^{-1}$ and the initial pH 2.50. The reaction went more slowly when the concentration was lower (4 mM) or higher (32 mM). At low concentration, H_2O_2 cannot generate enough $HO^{\bullet}$ radicals and the oxidation rate is logically slow. The increase of the oxidant concentration from 4 to 8 mM leads to an increase in the reaction rate, as expected, because more radicals will be formed. Nevertheless, for a very high H_2O_2 concentration (32 mM), the performance decreases.

Fig. 9 shows the effect of initial concentration of AR1 on the decolorization efficiency of AR1. It was observed that the higher

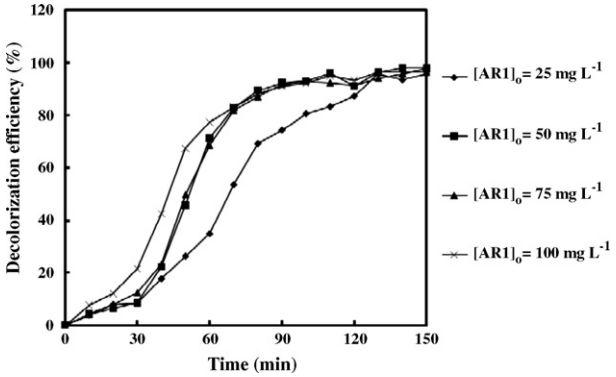

Fig. 9. Effect of AR1initial concentration on the decolorization of AR1. *Reaction conditions*: initial concentration of hydrogen peroxide, $[H_2O_2]_0 = 16\,mM$; dosage of catalyst = $5.0\,g\,L^{-1}$ with 0.14 wt.% of iron ions in catalyst; temperature = 30 °C; agitation speed = 130 rpm; and pH 2.5.

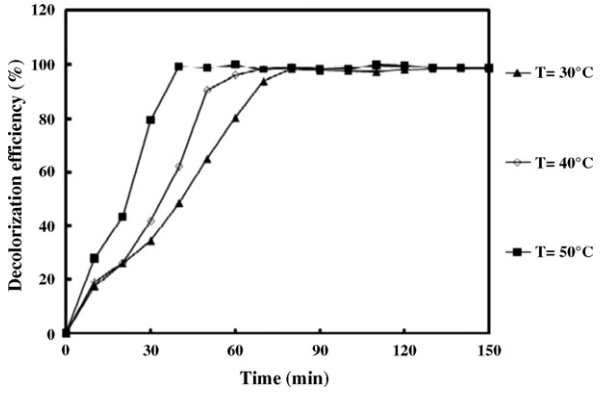

Fig. 10. Effect of temperature on the decolorization of AR1. *Reaction conditions*: initial concentration of AR1, $[AR1]_0 = 50\ mg\ L^{-1}$; initial concentration of hydrogen peroxide, $[H_2O_2]_0 = 16\ mM$; dosage of catalyst = $5.0\ g\ L^{-1}$ with 0.14 wt.% of iron ions in catalyst; agitation speed = 130 rpm; and pH 2.5.

the concentration of dye, the shorter is the reaction period needed to decolorize AR1 completely. As the lifetime of hydroxyl radicals is very short (only a few nanoseconds), they can only react where they are formed. Increasing the quantity of AR1 molecules per volume unit logically enhances the probability of collision between organic matter and oxidizing species, leading to an increase in the degradation efficiency [32].

The results obtained for the AR1 decolorization at three different temperatures (30 °C, 40 °C and 50 °C) are shown in Fig. 10. The results show clearly that the reaction rate increases with increase in temperature. This is because higher temperature increased the reaction rate between H_2O_2 and any form of ferrous/ferric ion, thus increasing the rate of generation of oxidizing species such as •OH radical or high-valence iron species. Similar results have been reported [33] where similar performances were achieved at higher temperatures due to the accelerated decomposition of H_2O_2 into oxygen and water.

3.4. Spectral changes of AR1 during decolorization process

The changes in the absorption spectra of AR1 solution during the decolorization process at different reaction times are shown in Fig. 11. As can be seen from the spectra, before the treatment, the UV–vis spectrum of AR1 was characterized by one main band in the visible region, with its maximum absorption at 532 nm, and by two bands in the ultraviolet region located at 322 nm and 354 nm. Different structural units and groups in the dye molecules have different absorbance peaks, the main conjugates of AR1 include azo linkage (–N=N–), benzene and naphthalene ring. The chromophore containing azo linkage has absorption in the visible region, while benzene and naphthalene ring have it in the ultraviolet region, and naphthalene ring's absorption wavelength is higher than that of the benzene ring [33]. It was clearly observed that the absorption peak at 532 nm diminished very fast and almost completely disappeared under 150 min of reaction. This indicated a rapid decolorization of AR1, a complete decolorization of $50\ mg\ L^{-1}$ AR1 can be achieved in 150 min in the presence of 16 mM H_2O_2 and $5.0\ g\ L^{-1}$ of catalyst. The ultraviolet band at 322 nm and 354 nm was also observed to gradually diminish but at a lower rate than that of visible band, which indicated the destruction of the benzene and naphthalene rings. Therefore, •OH radical first attacks azo groups and opens –N=N– bonds, destructing the long conjugated π systems and consequently causing decolorization [34].

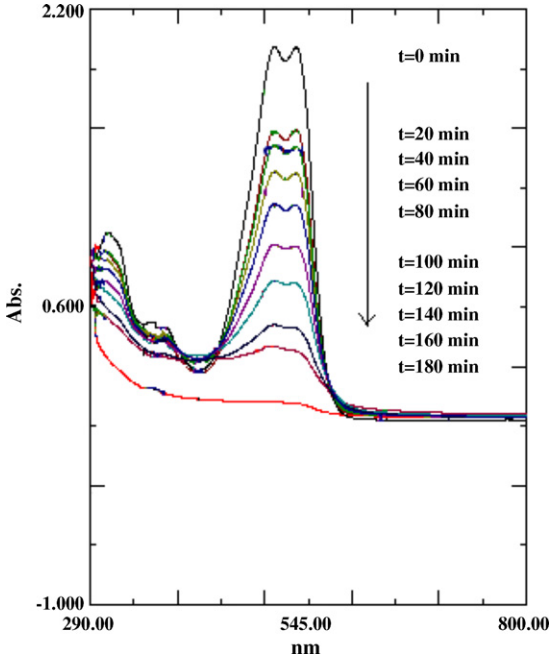

Fig. 11. Absorbance spectra. *Reaction conditions*: initial concentration of AR1, $[AR1]_0 = 50\ mg\ L^{-1}$; initial concentration of hydrogen peroxide, $[H_2O_2]_0 = 16\ mM$, dosage of catalyst = $5.0\ g\ L^{-1}$ with 0.14 wt.% of iron ions in catalyst, agitation speed = 130 rpm; temperature = 30 °C; and pH 2.5.

3.5. Catalyst stability and leaching test

Fig. 12 shows the performance reached in terms of AR1 decolorization in four consecutive cycles. To recover the catalyst, the final effluent was filtered. After the first cycle, and in order to check if the leached iron was responsible for the catalytic activity, both AR1 and H_2O_2 were added to the solution in the same concentrations at the beginning of the experiment. Fig. 12 shows that in these conditions AR1 decolorization is only a very small fraction of that recorded in the presence of the Fe–MK10. Although a homogeneous catalytic contribution also exists, as a consequence of the iron leaching, the process is essentially heterogeneous. For subsequent cycles, the filtered catalyst was dried overnight between consecutive runs. Even though slight activity decay was observed, this might be due to the iron loss, AR1 decolorization decreases from 99 to 64% in fourth cycles, i.e., 12 h of operation. Other authors reported similar results, but they attributed the loss of activity to poisoning of the active catalytic sites due to adsorbed organic species [30]. Leaching tests

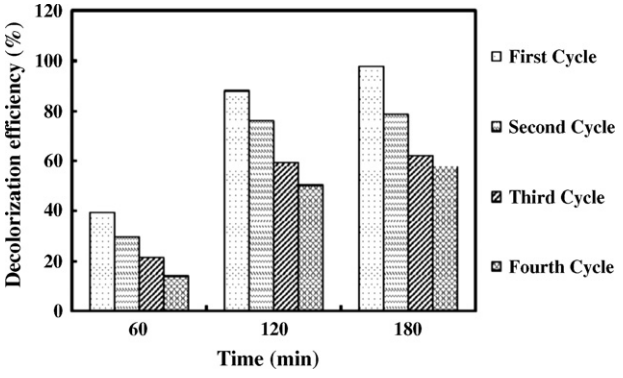

Fig. 12. Reusability test of the Fe–MK10. *Reaction conditions*: initial concentration of AR1, $[AR1]_0 = 50\ mg\ L^{-1}$; initial concentration of hydrogen peroxide, $[H_2O_2]_0 = 16\ mM$; dosage of catalyst = $5.0\ g\ L^{-1}$ with 0.14 wt.% of iron ions in catalyst; agitation speed = 130 rpm; temperature = 30 °C; and pH 2.5.

were carried out to check the potential of leaching of iron ions from MK10. In all of the experiments, concentration of the Fe ion was below 5 mg L^{-1} and this conforms to the standard of Environmental Quality (Sewage and Industrial Effluents) Regulation 1979.

4. Conclusion

In this study it was demonstrated that the Fe–MK10 obtained through impregnation method served as a reactive Fenton-like heterogeneous catalyst for the decolorization of AR1. Under the best conditions (0.14 wt.% Fe–MK10, 5.0 g L^{-1} dosage of catalyst, pH 2.5, 16 mM of H_2O_2), 99% decolorization of solution containing 50 mg L^{-1} AR1 could be removed within 150 min in a batch process. The Fe–MK10 catalyst exhibit not only good catalytic activity but also reasonable small iron leaching (below the Environmental Quality (Sewage and Industrial Effluents) Regulation 1979 values), indicating that the active phases are strongly fixed to the support (possibly iron strongly bonded to the surface of MK10 or engaged in small oxide clusters dispersed in the solid, inside or outside the porosity). Consecutive reaction cycles carried out with this sample showed a minor deactivation, which is possibly due to some iron leaching, thus evidencing the possibility of being used in continuous processes.

Acknowledgements

The authors acknowledge the research grant provided by Universiti Sains Malaysia, under short-term grant (Project No. 6039004) that has resulted in this article. The first author also acknowledges the financial support from National Science Fellowship (NSF), Ministry of Science, Technology and Innovation (MOSTI), Malaysia and Skim Penyelidikan Siswazah Universiti Penyelidikan (USM-RU-PRGS) grant (1001/PJKIMIA/8032040).

References

[1] C. Berberidou, I. Poulios, N.P. Xekoukoulotakis, D. Mantzavinos, Sonolytic, photocatalytic and sonophotocatalytic degradation of malachite green in aqueous solutions, Appl. Catal. B 74 (2007) 63–72.
[2] M.N. Timofeeva, S.T. Khankhasaeva, S.V. Badmaeva, A.L. Chuvilin, E.B. Burgina, A.B. Ayupov, V.N. Panchenko, A.V. Kulikova, Synthesis, characterization and catalytic application for wet oxidation of phenol of iron-containing clays, Appl. Catal. B 59 (2005) 243–248.
[3] V. Kitsiou, N. Filippidis, D. Mantzavinos, I. Poulios, Heterogeneous and homogeneous photocatalytic degradation of the insecticide imidacloprid in aqueous solutions, Appl. Catal. B 86 (2009) 27–35.
[4] F.L.Y. Lam, X. Hu, T.M.H. Lee, K.Y. Chan, A combined technique of photo-doping and MOCVD for the development of heterogeneous photo-Fenton catalyst, Sep. Purif. Technol. 67 (2009) 233–237.
[5] H. Kušić, A.L. Božić, N. Koprivanac, Fenton type processes for minimization of organic content in coloured wastewaters. Part 1. Processes optimization, Dyes Pigments 74 (2007) 380–387.
[6] A.S. Özcan, A. Özcan, Adsorption of acid dyes from aqueous solutions onto acid-activated bentonite, J. Colloid Interface Sci. 276 (2004) 39–46.
[7] I.D. Mall, V.C. Srivastava, N.K. Ararwal, I.M. Mishra, Removal of congo red from aquoes solution by bagasse fly ash and activated carbon: kinetic study and equilibrium isotherm analyses, Chemosphere 61 (2005) 492–501.
[8] S.L. Orozco, E.R. Bandala, C.A. Arancibia-Bulnes, B. Serrano, R. Suárez-Parra, I. Hernández-Pérez, Effect of iron salt on the color removal of water containing the azo-dye reactive blue 69 using photo-assisted Fe(II)/H_2O_2 and Fe(III)/H_2O_2 systems, J. Photochem. Photobiol. A 198 (2008) 144–149.
[9] M. Neamtu, I. Siminiceanu, A. Yediler, A. Kettrup, Kinetics of decolorization and mineralization of reactive azo dyes in aqueous solution by the UV/H_2O_2 oxidation, Dyes Pigments 53 (2002) 93–99.
[10] D. Hermosillaa, M. Cortijo, C.P. Huang, The role of iron on the degradation and mineralization of organic compounds using conventional Fenton and photo-Fenton processes, Chem. Eng. J. 155 (2009) 637–646.
[11] E. Rosales, M. Pazos, M.A. Longo, M.A. Sanromán, Electro-Fenton decoloration of dyes in a continuous reactor: a promising technology in colored wastewater treatment, Chem. Eng. J. 155 (2009) 62–67.
[12] T. Zhou, T.T. Lim, X. Lu, Y. Li, F.S. Wong, Simultaneous degradation of 4CP and EDTA in a heterogeneous Ultrasound/Fenton like system at ambient circumstance, Sep. Purif. Technol. 68 (2009) 367–374.
[13] I. Grčić, D. Vujević, N. Koprivanac, Modeling the mineralization and discoloration in colored systems by (US) $Fe^{2+}/H_2O_2/S_2O_8^{2-}$ processes: a proposed degradation pathway, Chem. Eng. J. 157 (2010) 35–44.
[14] C.S. Castro, M.C. Guerreiro, L.C.A. Oliveira, M. Goncalves, A.S. Anastácio, M. Nazzarro, Iron oxide dispersed over activated carbon: support influence on the oxidation of the model molecule methylene blue, Appl. Catal. A 367 (2009) 53–58.
[15] T.L.P. Dantas, V.P. Mendonça, H.J. José, A.E. Rodrigues, R.F.P.M. Moreira, Treatment of textile wastewater by heterogeneous Fenton process using a new composite Fe_2O_3/carbon, Chem. Eng. J. 118 (2006) 77–82.
[16] M.B. Kasiri, H. Aleboyeh, A. Aleboyeh, Degradation of Acid Blue 74 using Fe-ZSM5 zeolite as a heterogeneous photo-Fenton catalyst, Appl. Catal. B 84 (2008) 9–15.
[17] A. Durán, J.M. Monteagudo, E. Amores, Solar photo-Fenton degradation of Reactive Blue 4 in CPC reactor, Appl. Catal. B 80 (2008) 42–50.
[18] L.C.A. Oliveira, M. Gonçalves, M.C. Guerreiro, T.C. Ramalho, J.D. Fabris, M.C. Pereira, K. Sapag, A new catalyst material based on niobia/iron oxide composite on the oxidation of organic contaminants in water via heterogeneous Fenton mechanisms, Appl. Catal. A 316 (2007) 117–124.
[19] J. Deng, J. Jiang, Y. Zhang, X. Lin, C. Du, Y. Xiong, $FeVO_4$ as a highly active heterogeneous Fenton-like catalyst towards the degradation of Orange II, Appl. Catal. B 84 (2008) 468–473.
[20] C.P. Huang, C. Dong, Z. Tang, Advanced chemical oxidation: its present role and potential future in hazardous waste treatment, Waste Manage. 13 (1993) 361–377.
[21] T. Zhou, Y. Li, J. Ji, F.S. Wong, X. Lu, Oxidation of 4-chlorophenol in a heterogeneous zero valent iron/H_2O_2 Fenton-like system: kinetic, pathway and effect factors, Sep. Purif. Technol. 62 (2008) 551–558.
[22] N.K. Daud, B.H. Hameed, Decolorization of Acid Red 1 by Fenton-like process using rice husk ash-based catalyst, J. Hazard. Mater. 176 (2010) 938–944.
[23] N.K. Daud, B.H. Hameed, Fenton-like oxidation of reactive black 5 solution using iron–Montmorillonite K10 catalyst, J. Hazard. Mater. 176 (2010) 1118–1121.
[24] Y. Flores, R. Flores, A.A. Gallegos, Heterogeneous catalysis in the Fenton-type system reactive black 5/H_2O_2, J. Mol. Catal. A: Chem. 281 (2008) 184–191.
[25] S. Gopinath, S. Sugunan, Enzymes immobilized on motmorillonite K10 effect of adsorption and grafting on the surface properties and the enzyme activity, Appl. Clay Sci. 35 (2007) 67–75.
[26] Q. Chen, P. Wu, Y. Li, N. Zhu, Z. Dang, Heterogeneous photo-Fenton photodegradation of reactive brilliant orange X-GN over iron-pillared montmorillonite under visible irradiation, J. Hazard. Mater. 168 (2009) 901–908.
[27] F. Martínez, G. Calleja, J.A. Melero, R. Molina, Heterogeneous photo-Fenton degradation of phenolic aqueous solutions over iron-containing SBA-15 catalyst, Appl. Catal. B 60 (2005) 181–190.
[28] F. Martínez, G. Calleja, J.A. Melero, R. Molina, Iron species incorporated over different silica supports for the heterogeneous photo-Fenton oxidation of phenol, Appl. Catal. B 70 (2007) 452–460.
[29] F.G.E. Nogueira, J.H. Lopes, A.C. Silva, M. Gonçalves, A.S. Anastácio, K. Sapag, L.C.A. Oliveira, Reactive adsorption of methylene blue on montmorillonite via an ESI-MS study, Appl. Clay Sci. 43 (2009) 190–195.
[30] J.H. Ramirez, C.A. Costa, L.M. Madeira, G. Mata, M.A. Vicente, M.L. Rojas-Cervantes, A.J. López-Peinado, R.M. Martín-Aranda, Fenton-like oxidation of Orange II solutions using heterogeneous catalysts based on saponite clay, Appl. Catal. B 71 (2007) 44–56.
[31] J. Feng, X. Hu, P.L. Yue, H.Y. Zhu, G.Q. Lu, Degradation of azo-dye orange II by a photoassisted Fenton reaction using a novel composted of iron oxide and silicate nanoparticles as a catalyst, Ind. Eng. Chem. Res. 42 (2003) 2058–2066.
[32] E.G. Solozhenko, N.M. Soboleva, V.V. Goncharuk, Decolourization of azodye solutions by Fenton's oxidation, Water Res. 29 (1995) 2206–2210.
[33] J. Chen, I. Zhu, Heterogeneous UV-Fenton catalytic degradation of dyestuff in water with hydroxyl-Fe pillared bentonite, Catal. Today 126 (2007) 463–470.
[34] Y. Zhang, X. Dou, J. Liu, M. Yang, L. Zhang, Y. Kamagata, Decolorization of reactive brilliant red X-3B by heterogeneous photo-Fenton reaction using an Fe–Ce bimetal catalyst, Catal. Today 126 (2007) 387–393.